Defence Science Journal, Vol. 74, No. 5, September 2024, pp. 713-721, DOI : 10.14429/dsj.74.19779

Optimized Mosaic Method for Accurate Measurement of Soot Concentration: Indirect Method

Ratko Ivković

Department of Information Technology, MB University, Prote Mateje br. 21, 11111 Beograd, Serbia
E-mail: ratko.ivkovic@pr.ac.rs

ABSTRACT

Global air pollution poses health risks. Soot is a major contributor to warming and pollution. Measuring soot is key to mitigating emissions. This study proposes an empirical method using markers to indirectly gauge soot levels. The Mosaic method was tested against conventional techniques with over 50 samples. This method utilizes markers to collect impurities in the air, employing the μ/m³, m(g), and the newly devised Mosaic method. All results underwent standard statistical processing, enabling a comparison between the new method (Mosaic) and conventional techniques used.

Keywords: Digital image processing; Hybrid method; Mosaic method; Soot measurement

1. INTRODUCTION

One of the models employed for assessing environmental changes involves visual measurements. Utilizing an optical sensor allows for versatile presentations of environmental alterations, with wide-ranging applications[1-6]. Despite the optical sensor's inclination to capture perspectives akin to human perception, image recording methods can be tailored to diverse research requirements[7-8]. Advanced algorithms, digital image processing techniques, and various sensors enable the detection and numerical representation of specific aspects of the surrounding environment[9-12]. The measurement of air pollution poses a substantial challenge across scientific disciplines. Beyond visually representing global air pollution, the numerical presentation of results holds paramount importance. This manuscript constitutes a contribution to epidemiology, specifically in the realm of measuring soot concentration in markers. Soot encompasses various toxic substances that can induce respiratory issues, particularly exacerbating health conditions in individuals with pre-existing respiratory ailments. Numerous studies indicate that soot particles are frequently carcinogenic. While short-term exposure to soot inhalation may not register a significant impact on health, prolonged exposure yields detrimental effects on the organism. Therefore, this 24 hrs study aims to illustrate potential human exposure to soot at the specified location[13]. The measurement of soot concentration through the reflection method is grounded in assessing incident and reflected radiation concentrations relative to the marker surface. This method is considered a reference standard for measuring soot concentration[14-16]. Alternatively, measuring soot concentration via electronic scales involves gauging the weight difference between the marker sample before and after placement on the measuring station. The disparity in marker weight before and after measurement completion denotes the concentration of soot, typically expressed in micrograms[14-16]. Markers, which accumulate soot particles, are positioned on measuring stations and retrieved after 24 hrs from designated measurement points. Markers were collected from seven different locations. The locations have been selected to cover seven different city zones, from the city centre to the outskirts. This range of values and number of samples provided a quality basis as a benchmark for the new method. The measurement period is one week, so the markers are an indicator of pollution at specific locations during one week of city life.

Recent research has focused on the developmental applications of computer vision and image processing in various fields. For instance, Gu[17], *et al.* proposed a visual system for monitoring soot emissions from flares in the petrochemical industry, which combines flame detection, saliency segmentation, and color processing for soot identification. Manoel[18], *et al.* developed a colorimetric determination of hydrogen peroxide as a contaminant in milk using digital images and photometry on a smartphone. Oveis[19], *et al.* devised a method for measuring the chlorophyll content in soybean leaves using a smartphone camera, image processing, and machine learning, thereby circumventing the costly SPAD method and destructive sampling. Zhao[20], *et al.* highlighted challenges in using a canopy cover for assessing nitrogen status in wheat, indicating the need for further research and improvements. These works underscore the advantages of computer vision and digital image-based approaches, such as simplicity, portability, and minimal sample and reagent consumption.

Today, there is a high degree of diffusion of the scientific field of computer vision, as evidenced by the aforementioned works employing digital images and processing for various

Received : 04 January 2024, Revised : 14 June 2024
Accepted : 08 July 2024, Online published : 19 September 2024

analytical purposes. However, there is no similar method for measuring soot concentration using computer vision, which constitutes the main advantage of this manuscript. The proposed procedure offers numerous advantages - sample and reagent consumption are minimized, the procedure is fast, inexpensive, and non-destructive compared to conventional techniques. Additionally, the method leverages the benefits of advanced algorithms for digital image processing, such as segmentation, edge detection, and filtering, enabling precise indirect quantification of soot. Furthermore, the proposed approach is portable and adaptable, making it suitable for use in various scenarios and industrial environments where measuring soot concentration is necessary. Overall, this method represents an efficient and cost-effective solution for soot monitoring, contributing to efforts to protect the environment and human health.

2. BACKGROUND

The development of precise and efficient techniques for measuring soot concentration holds significant relevance in defence science research. Soot emissions can impede visibility, disclosing the position of military vehicles, aircraft, and operations. Quantifying soot levels allows for assessing potential exposure risks for soldiers and evaluating impacts on operational security. Additionally, measuring soot concentration contributes to assessing the environmental effects of defence activities. Refined methods for determining soot concentrations are essential for various military applications. Diesel engines, commonly used in combat vehicles and engineering systems due to their reliability and fuel efficiency, produce high levels of soot emissions. Accurate quantification of soot output from military diesel engines facilitates optimization to balance power and emissions management. Precise measurement of aircraft engine emissions is crucial, as soot accumulation can degrade performance. Monitoring soot levels enables early detection of potential issues. Armaments and explosives produce significant soot when detonated, obstructing vision and impeding operations.

Fast and accurate techniques for measuring soot concentration from detonations provide tactical awareness of the battlefield environment. Soot measurement aids in assessing detonation performance and effects. Advancing soot measurement techniques aligns with key defence science priorities in propulsion, armaments, and biomedical monitoring. The demonstrated performance of the Mosaic method indicates utility across multiple military domains. Further refinement and validation of the approach through additional testing with defence systems and conditions would maximize its relevance and impact for the defence research community. The capability to accurately and efficiently quantify soot levels will aid in engineering design, health surveillance, and tactical operations.

3. METHODOLOGY

3.1 Mosaic Method Optimised for Measuring Soot Concentration in Markers

Mosaic method undergoes a direct comparison with two commonly utilised methods, where the accuracy is contingent on the measuring instruments employed. Reflection method is

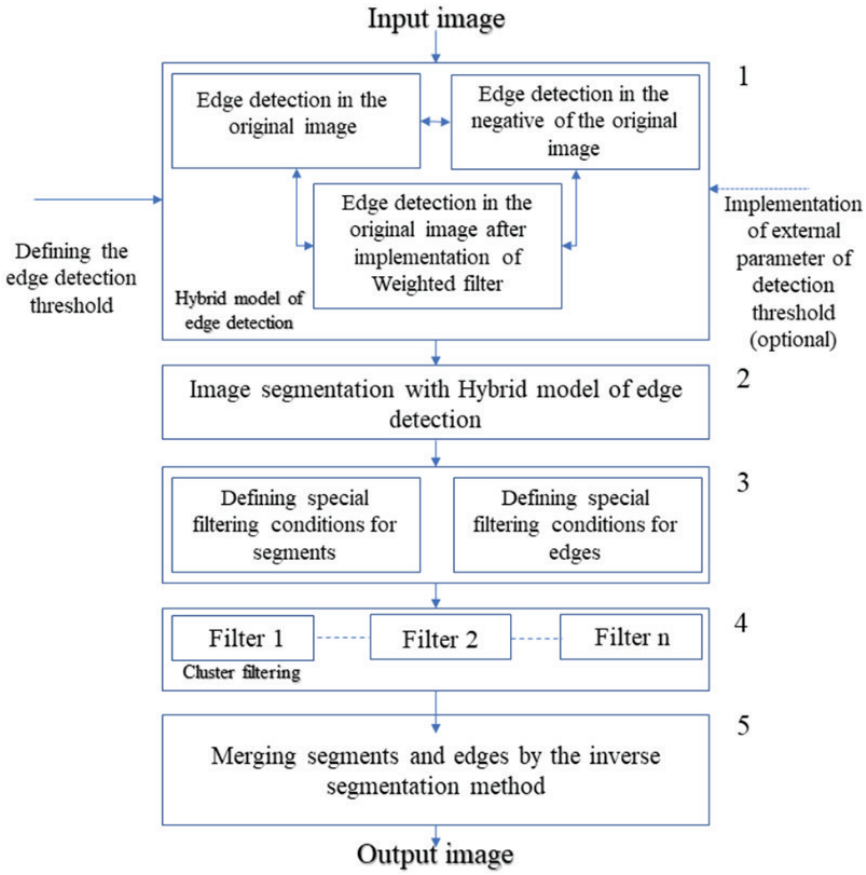

Figure 1. Algorithm of mosaic methods.

grounded in the AVL 415SE Measurement Principle, while the Electronic Scales method relies on Kern & Sohn ABJ 120-4 M. The Mosaic method represents a digital image processing approach optimised for both grayscale and RGB color systems. This proposed method involves the independent processing of segments and edges within a digital image. To mitigate boundary condition errors, the processing is conducted based on detection without overlap, ensuring that all pixels are processed without repetition via the Mosaic method[21]. The dimensions of the segments are variable, ranging from 1x1 pixels to several hundred pixels, depending on the defined segments. Grayscale levels define the edges, allowing users to set a detection threshold for enhanced edge detection accuracy. The detected edges serve as the foundation for segment extraction. Cluster filtering, employing specifically defined conditions, is then applied to the separated segments and edges, followed by their merging. The entire process comprises seven blocks, as illustrated in Fig. 1.

3.2 Grayscale or RGB Image

The image preparation method in which the image is treated as grayscale level increases the degree of edge detection accuracy, when it comes to images where shades of gray dominate. All images in this study were generated in 8-bit and 16-bit technique using a Sony Alpha series digital camera with a CMOS optical sensor.

3.3 Weighted Filter

There are various modifications of median filter, based on the matrix pixels approximation[22]. The most popular among them are the filter of medium value (average filter) and weighted filter. The difference between above mentioned filter is comprised in a different defined sub-matrix, as well as pre-multiplier of the sub-matrix[23]. For the weighted filter:

$$wt = \frac{1}{4}\begin{bmatrix} 1 & 2 & 1 \\ 2 & 4 & 2 \\ 1 & 2 & 1 \end{bmatrix} \quad (1)$$

For this manuscript an important characteristic of this filter is to be used for the noise in the image of up to 5 %, as shown in research work[24].

3.4 Hybrid Edge Detection Model

Optical sensor imperfections and the transformation of the visual spectrum into an electrical signal are the first digital image noise generators. Although technology has advanced far, this process is still imperfect and introduces a certain degree of noise into the image[25-26]. This model allows the edges of the digital image to be extracted with precise control of the detection threshold controlled by the user.

The output image as a result of Hybrid Method of Edge Detection processing[26] is defined as the full processing result over the original image, the original image negative and the Weighted filter with a detection threshold of 13. The detection threshold is defined in relation to gray scale and defined at 5 % of scale. Edge detection in the case of 5 % detection is close to the characteristics of the Sobel operator, however, in the case of nanoparticle images there is a certain degree of increased

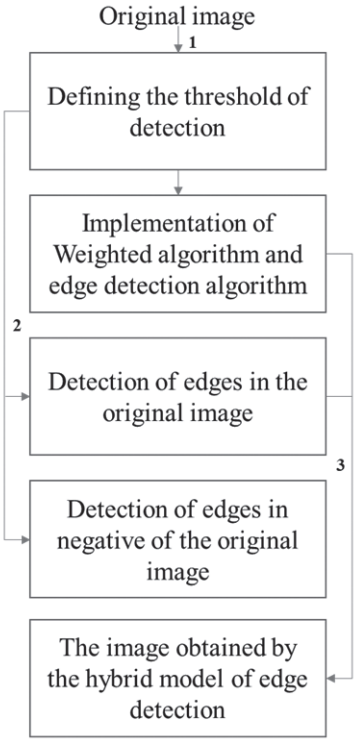

Figure 2. Block diagram of hybrid method of edge detection.

noise that needs to be eliminated before edge detection. For this reason, the Hybrid Model is an excellent solution for nanoparticle detection. The hybrid method already includes a Weighted filter that is used to reduce up to 5 % of noise, and with the detection threshold control, the detection process can be further controlled. Figure 2 shows a block diagram of the Hybrid method of Edge Detection. The loading of the image and the definition of the detection threshold are indicated with the number 1. Number 2 indicates the parts of the code in which the edge detection is performed. At the very end, in the part of the code marked with the number 3, the intermediate results of edge detection over the original image, the negative of the original image and the Weighted filter are combined with a detection threshold of 13. Regardless of the technology, the process of generating the image is not immune to noise, so algorithms with a low threshold for detecting edges perceive noise as edges. In the hybrid image edge detection model, edge detection is performed by comparison through three completely independent processes of measuring the change in the value of adjacent pixels in order to eliminate the effect of error, namely:

- The image processed by the Weighted algorithm.
- The image negative processed by the Weighted algorithm.
- The original grayscale image after applying the supplementary algorithm.

The comparison process shown in[21] speaks of a triple comparison with respect to the initial detection, pixel "X". Comparison of pixel „X" with pixel values in the grayscale at positions "X_1, X_2 and X_3" increases the detection accuracy relative to the 2D gradient for additional "X_3" digital comparison. The comparison is also made over the negative of the image and added to the obtained values. In this way,

the errors that occur under the boundary conditions of edge detection are significantly reduced. The final result is an image of the sum of the results of the three treatments.

3.5 Segmentation

After hybrid edge detection, the image is divided into separate segments bounded by the detected edges. These segments represent distinct regions in the image that need to be processed individually. Since the edges carry critical information, special care is taken in processing the edge segments. The areas of the digital image located between the detected edges form the non-edge segments. Each of these non-edge segments is treated as a separate unit to be analysed.

For the edge segments, additional processing steps are applied:

- Edge linking and completion: Any broken, discontinuous edges are linked together and closed contours are formed around each distinct object/region.
- Edge thinning: The edge segments are thinned to single pixel width using morphological operations to obtain accurate boundary representation.
- Segment labeling: Each closed edge contour is assigned a unique label, and the corresponding region inside that contour also gets the same label, allowing individual processing.
- Filtering small segments: Very small segments below a specified size threshold are filtered out as noise/irrelevant regions.

After this processing of edges and labeling of segments, each distinct segment (both non-edge and edge-bounded) can be analyzed independently based on properties like color, texture, shape etc. This allows relevant segments containing the markers to be identified and extracted for subsequent soot concentration measurement.

3.6 Defining Special Conditions

Special filtering conditions can depend on the detail level values of each segment separately, standard deviation, color value, required object in the image and many other conditions, depending on the specifics of the situation.

3.7 Cluster Filtering

Synchronised filtering of two or more applied filters over the original image gives the result of processing with this type of filtering. However, in the case of measuring soot concentration in markers, filters will not change the color values, but will select the pixels representing the marker region based on their colors.

For instance, typical special conditions that can be defined are the ranges of values for the red (R), green (G), and blue (B) components for brown shades that represent soot stains on markers. The upper and lower threshold values of the R, G, and B components can be adjusted to encompass the range of brown colors caused by soot contamination, while excluding other colors such as red, blue, green, etc. This color-based segmentation helps isolate only the regions of interest on the marker surface. Another example could be defining a certain range of greyscale values to select pixels within that range which correspond to the brown color of soot stains, while eliminating lighter/darker shades of other molecules present in the sample media. The defined conditions primarily aim to separate and extract the relevant image regions containing soot information from the background/substrate signal of markers or solutions applied for that particular application. This extracted data can then be quantified and analysed.

Values after marker processing by the Mosaic method are expressed in grayscale. In this way, the results of Mosaic processing will be indirectly connected with the values of soot concentration. Whatman filter paper for measuring soot before the start of the measurement and after the end of the measurement are shown in Fig. 3.

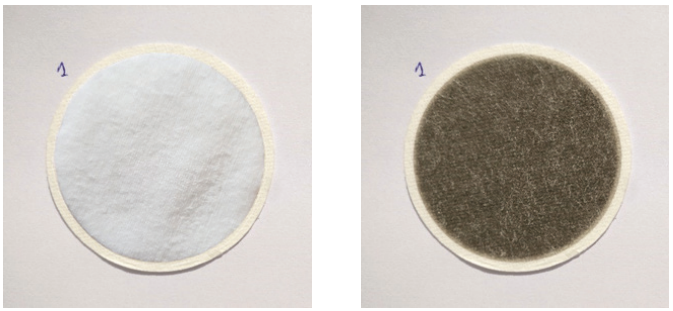

(a) (b)

Figure 3. Marker for measuring soot concentration: (a) Before measurement, and (b) After measurement.

3.8 Mosaic Method Optimized for Measuring Soot Concentration in Markers

After taking the marker from the measuring location, the marker was subjected to measurements by the reflection method, the electronic scale method and the mosaic method. The mosaic method optimized for measuring the concentration of soot was realized through the following procedures:

- A hybrid segmentation process in which a marker is separated from the rest of the image.
- Defining special conditions, which eliminate errors that occur as a consequence of fiber imperfections in markers.
- Measurement of color (grayscale) concentration in the marker.
- Representation of a number of values through a grayscale.

All images are generated in a TIFF-free compression format, so that the impact of compression is reduced. In this way, it is reduced that compression errors affect the final result. Images are stored in 8-bit and 16-bit grayscale format. On Fig. 4, images depicting part of different markers are presented after the measurement has been conducted. The markers are placed on a background that gives a high contrast (white color) in relation to the color after the measurement in order to be more of a precise segmentation. After recording, the algorithm separated the image segments with a tolerance of 50[27]. A view of the separate segments after the first step can be seen in Fig. 6.

The second step is to eliminate the error caused by the imperfection of the fibers in the marker. This is necessary to

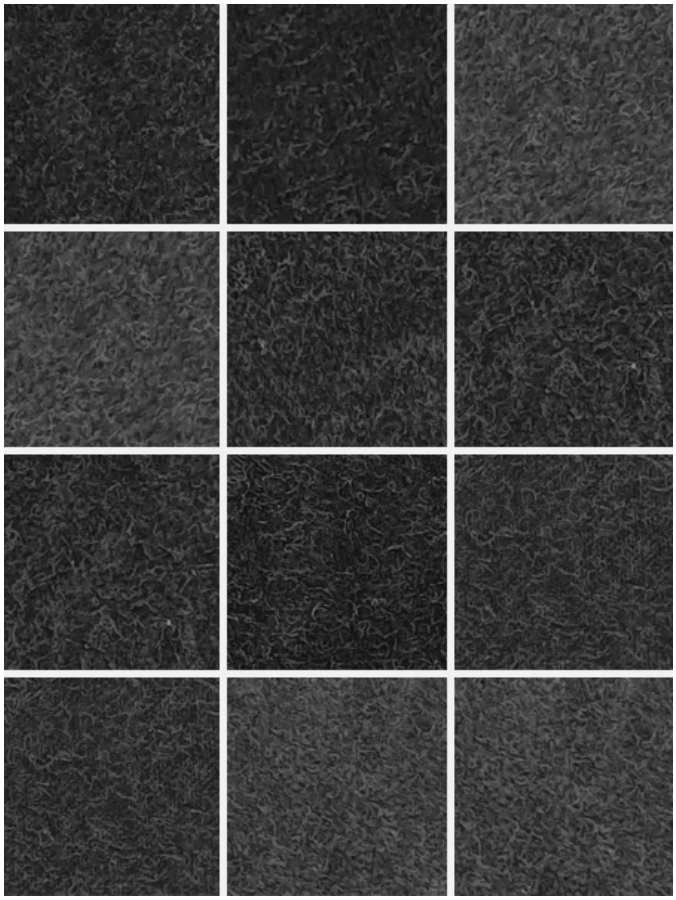

Figure 4. Images of part of different markers.

Figure 5. Images of markers after applying the Mosaic method.

Figure 6. Negative image of the marker with the correction of impurities.

even out the color of the marker, because the surface of the marker is not completely homogeneous. Namely, certain parts of the markers did not receive soot particles during the measurement, so it is desirable to eliminate as high a percentage of these marker elements as possible. In this case, a hybrid edge detection method with a detection threshold of 7 is used, in order to define all areas that will not be included in the analysis, Figure 7 shows the marker elements that were not subjected to analysis. Due to the better display, Figure 6 is shown in negative.

The pixels within the marker segment, as defined above, underwent color concentration measurement, method interrelationship assessment, and determination of standard deviation[26-29]. The correlation between the methods will elucidate the consistency of results for the observed markers, while the standard deviation will elucidate the percentage error between the mean values of the observed methods, as outlined in previous manuscripts[26-27]. Figure 7 illustrates the entire process, encompassing the extraction of the useful image segment, segregation of the unnecessary marker parts, and preparation for measuring grayscale concentration. Notably, the simplicity of the procedure lies in the fact that the marker image comprises only three segments (Fig. 7(b), (c) and (d)). Among these segments, only segment Figure d) undergoes the calculation of mean gray concentration values[25-27].

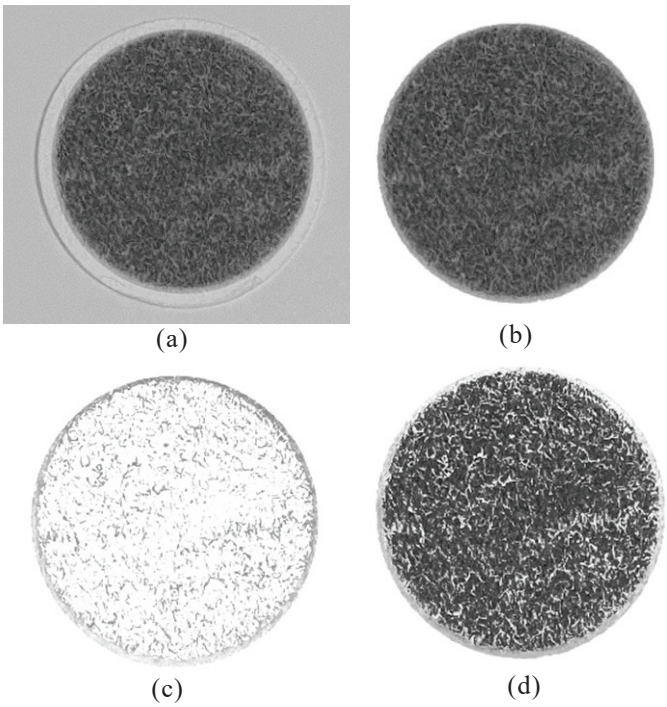

Figure 7. Mosaic method for measuring soot concentration: (a) Marker after measurement, (b) Extracting the useful part of the image segment, (c) Separating the unnecessary part of the marker and (d) Preparation for measuring the concentration of the grayscale.

4. RESULTS

The results of measurements obtained through the reflection method, electronic scales method, and soot via the indirect mosaic method are depicted in Graphs 1a, 1b, and 1c, respectively. The x-axis represents the values of

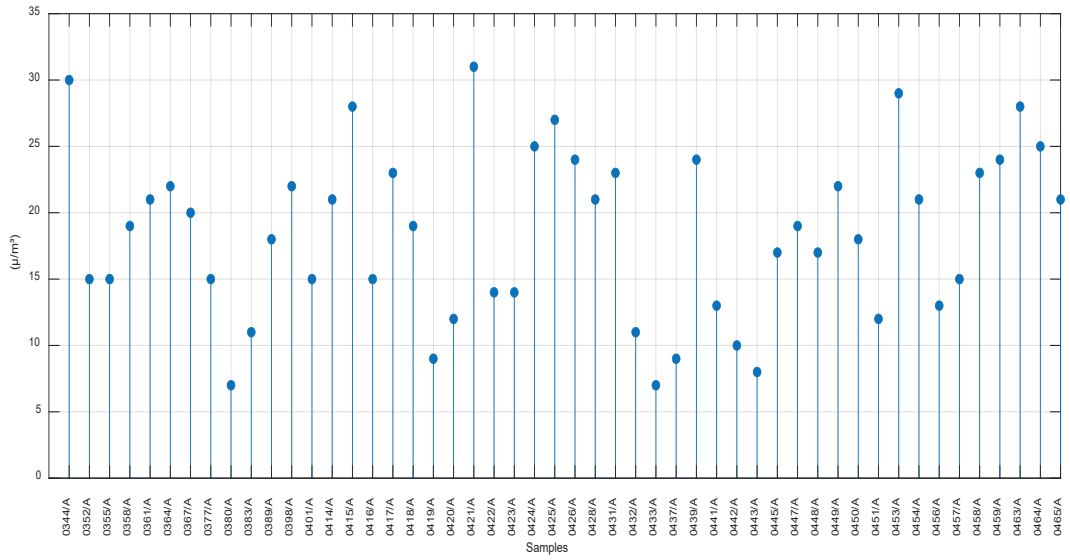

(a)

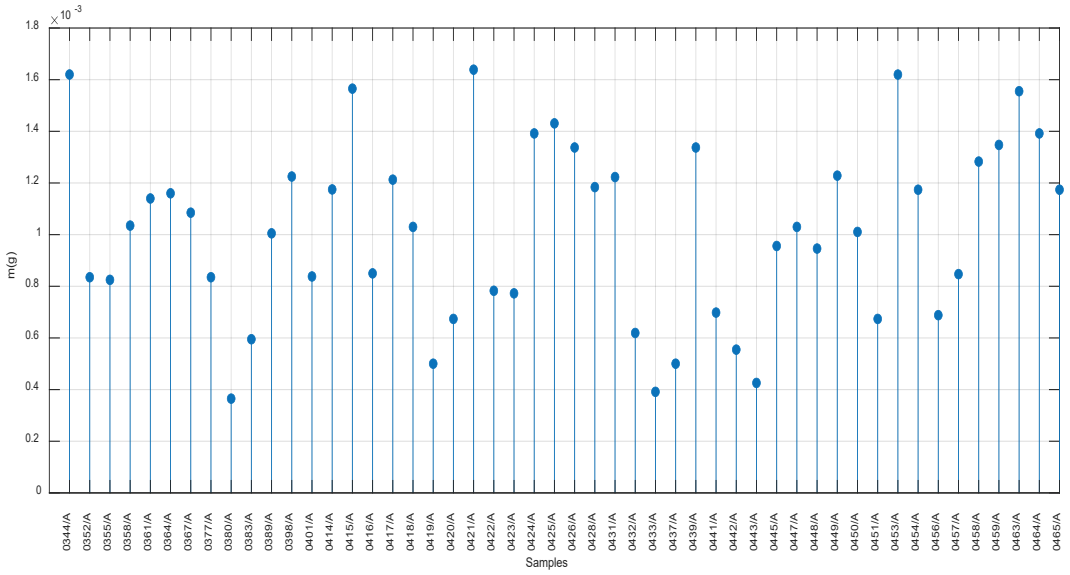

(b)

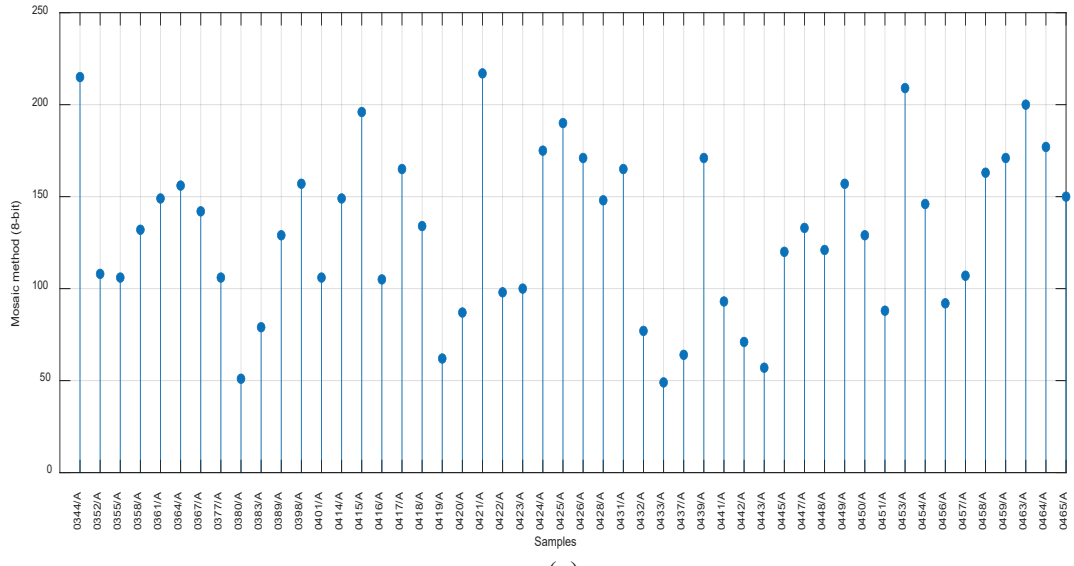

(c)

Figure 8. Results of measuring the concentration of soot: (a) By the method of reflection; b) With an electronic scale; (c) By the Mosaic method (8-bit).

the measured marker samples, while the y-axis displays the values of the samples in relation to the respective observed method. Graphs 1a and 1b illustrate outcomes obtained from established methods, whereas Graph 1c illustrates the results of the mean color value in the marker measured using the Mosaic method. The data extracted from Graphs 1a, 1b, and 1c affirm that the values of the measured samples align with each other. Notably, samples 0344/A, 0415/A, 0421/A, and 0454/A exhibit maximum values across all three graphs, while samples 0380/A, 0419/A, 0437/A, and 0443/A display the lowest values on all graphs. These outcomes signify the imperative need for a direct comparison of values between the two methods to ascertain their similarity and correlation.

Due to the enhanced precision of the proposed method, samples were independently recorded using both 8-bit and 16-bit techniques. In addition to the graphical representations in Graphs 2, 3, and 4, numerical results from the three methods are presented in Table 1 (in Appendix). The Mosaic method measurements were conducted utilizing two grayscale scales, specifically the 8-bit image format (comprising 256 levels of gray) and the 16-bit image format (comprising 65,536 levels of gray). The number of gray levels in the Mosaic method corresponds to the concentration levels of soot in the marker.

Thus, the 8-bit image recording allows for the capture of 256 distinct concentrations of soot, while the 16-bit recording expands this capability to 65,536 different concentrations of soot. The standard deviation of the relationship between the 8-bit and 16-bit methods serves as an indicator of the stability and precision of the proposed method. A low standard deviation value suggests negligible differences in the results of the samples between the two methods. In this study, the standard deviation for the 8-bit and 16-bit ratio yielded a value of 0.033307197. This value is inconsequential relative to the number of samples and their values. Furthermore, the Mosaic method (8-bit) offers the additional benefit of approximately threefold memory savings per sample. Consequently, the 8-bit measurement method can be employed with a high degree of accuracy.

5. DISCUSSION

A straightforward division of the obtained results elucidates the correlation between the two observed methods. If this ratio demonstrates approximately constant values, it indicates a correlation between the methods. The normalised deviation, serving as a measure of variation, expresses the algebraic deviation of the observed value from the arithmetic mean in terms of standard deviations. This measure is particularly useful for comparing variations in features from distinct numerical series expressed in different units of measure. Graph 2 displays standard deviation values among the observed methods, indicating that the most robust correlation is observed in the relationship between the Mosaic method and the reflection method, with a standard deviation of 0.08615269.

The results depicted in Graph 3 distinctly highlight the optimal relationship between the Mosaic method's indirect measurement of soot concentration and the reflection method. The maximum deviation observed between these two

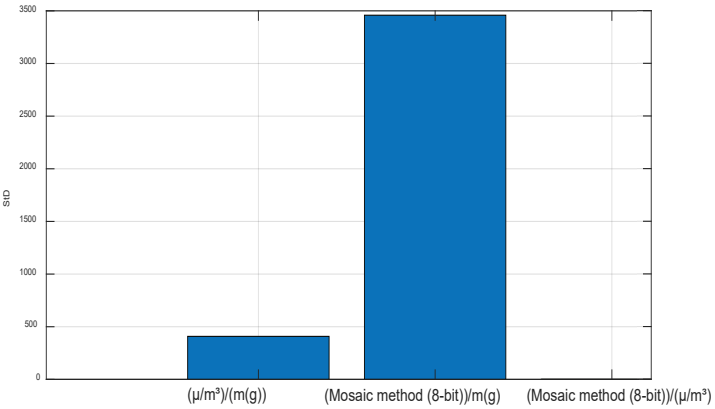

Figure 9. The relationship of standard deviation between the observed methods.

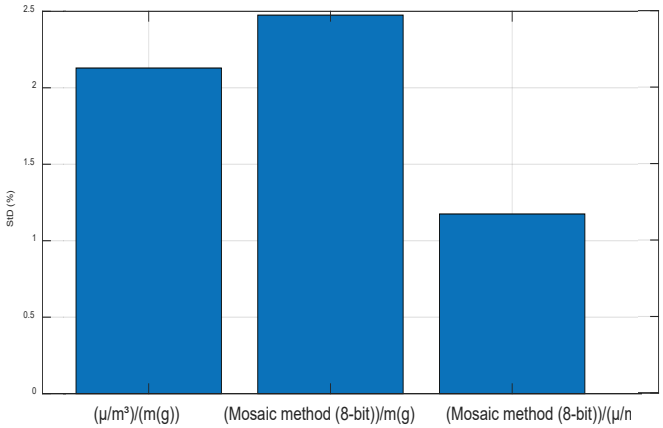

Figure 10. Values of standard deviation between methods in per cent.

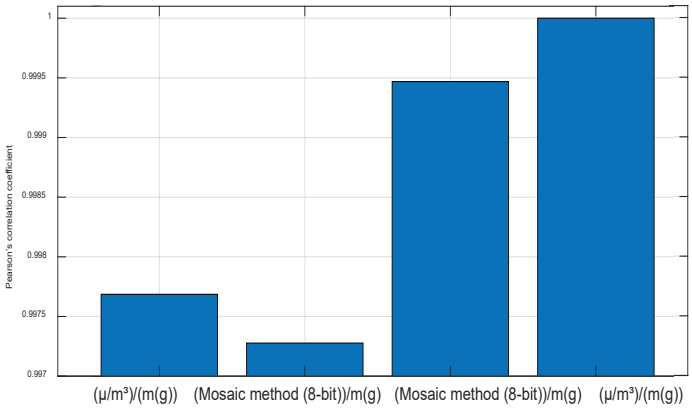

Figure 11. Pearson's correlation coefficient between observed methods.

methods is 1.174 %, whereas between the reflection method and electronic scales method, this ratio is nearly twice as substantial, amounting to 2.129 %.

Additional evidence of the stability of the proposed method is presented in Graphs 4. Pearson's correlation coefficient between the observed methods consistently approaches a value of 1 in all three scenarios. A value close to 1 signifies a remarkably high degree of synchronization in measurement samples across different methods. The correlation coefficient confirms that the smallest deviation between two methods is observed in the relationship between the Mosaic Method (8-bit) and the reflection method.

6. CONCLUSIONS

This paper introduces an optimised Mosaic method designed for the indirect measurement of soot concentration in markers. The method integrates the reflection method and electronic scale measurements, employing distinct measurement methodologies. Experimental values from these two methods are leveraged for the proposed approach, revealing a negligible difference of approximately 3 % in result accuracy. The optimized Mosaic method offers notable advantages over existing soot concentration measurement methods. These attributes render the Mosaic method an appealing choice for soot concentration measurement. The reflection method, serving as the standard for the Mosaic method's indirect measurement of soot concentration, involves a multiplier of around 7.1. This multiplier serves as the conversion factor for determining soot concentration based on reflection measurements. Additionally, the tolerance associated with the reflection method is approximately 1.174 %, representing an acceptable range of error in determining soot concentration.

Proposed Mosaic method, optimized for measuring soot concentration, exhibits enhanced efficiency and cost-effectiveness in comparison to existing methods.

REFERENCES

1. Arthur, H.L. A novel method of atomization with potential gas turbine applications. *Def. Sci. J.*, 2014, **38**, 355-360. doi: 10.14429/dsj.38.5869
2. Jia, L.; Muhammad K.; Qianlong W.; Ting L.; Haifeng L. & Mingfa Y. BPNN model based AI for the estimation of soot data from flame luminosity emissions in H2/N2 diluted ethylene laminar diffusion flames. *Experim. Thermal and Fluid Sci.*, 2024, **151**, 111072. doi:10.1016/j.expthermflusci.2023.111072
3. Pi, Z.; Zhou, Z.; Li, X. & Wang, S. Digital image processing method for characterization of fractures, fragments, and particles of soil/rock-like materials. *Mathematics*, 2021, **9**, 815. doi:10.3390/math9080815
4. Zhicong, L.; Chun, L. & Chun, Z. Investigation of structure and soot formation in laminar inverse diffusion flames by atomic ratio measurements using laser-induced breakdown spectroscopy. *Combustion and Flame*, 2023, **254**, 112870. doi: 10.1016/j.combustflame.2023.112870
5. Zielewska-Büttner, K.; Adler, P.; Kolbe, S.; Beck, R.; Ganter, L.M.; Koch, B. & Braunisch, V. Detection of standing deadwood from aerial imagery products: Two methods for addressing the bare ground misclassification issue. *Forests*, 2020, **11**, 801. doi:10.3390/f11080801
6. Liu, Q.; Chu, B.; Peng, J. & Tang, S. A visual measurement of water content of crude oil based on image grayscale accumulated value difference. *Sensors*, 2019, **19**, 2963. doi:10.3390/s19132963
7. Ivković, R.; Petrović, M.; Jakšić, B. & Cerić, V.; Milošević, M. Digital image fundaments through visible spectrum. *In* Zbornik radova XV međunarodnog naučno-stručnog simpozijuma INFOTEH 2016, Jahorina, Elektrotehnički fakultet, Istočno Sarajevo, Bosnia i Hercegovina, 2016.
8. Ivković, R.; Milošević, I.; Petrović, T.; Bijelović, S. & Ivković, N. Analiza kvaliteta različitih formata digitalne slike, međunarodna naučna konferencija Univerziteta Singidunum, SINTEZA 2015, Univerzitet Singidunum, Belgrade, Serbia, 2015. doi:10.15308/Synthesis-2015-171-175
9. Forestieri, S.D.; Helgestad, T.M.; Lambe, A.T.; Renbaum-Wolff, L.; Lack, D.A.; Massoli, P.; Cross, E.S.; Dubey, M.K.; Mazzoleni, C.; Olfert, J.S.; Sedlacek III, A.J.; Freedman, A.; Davidovits, P.; Onasch, T.B. & Cappa, C.D. Measurement and modeling of the multiwavelength optical properties of uncoated flame-generated soot. *Atmospheric Chem. Physic.*, 2018, **18**(16), 12141–12159. doi:10.5194/acp-18-12141-2018
10. Mehlman, M.A. Health effects and toxicity of phosgene: Scientific review. *Def. Sci. J.*, 2014, **37**, 275. doi: 10.14429/dsj.37.5909
11. Sacchis Lopes, M.; Kozhikkodan Veettil, B. & Saldanha, D.L. Assessment of small-scale ecosystem conservation in the Brazilian Atlantic forest: A study from Rio Canoas State Park, Southern Brazil. *Sustainability*, 2019, **11**(10), 2948. doi:10.3390/su11102948
12. Mishra, V.D. Albedo Variations and surface energy balance in different Snow-Ice Media in Antarctica, *Def. Sci. J.*, 2013, **49**, 355-362. doi: 10.14429/dsj.49.3849
13. Stylogiannis, A.; Kousias, N.; Kontses, A.; Ntziachristos, L.; Ntziachristos, V. A low-cost optoacoustic sensor for environmental monitoring. *Sensors*, 2021, **21**, 1379. doi:10.3390/s21041379
14. Dalzell, W.H.; Williams, G.C. & Hottel, H.C. A light-scattering method for soot concentration measurements. *Combustion and Flame*, 1970, **14**(2), 161-169. doi:10.1016/S0010-2180(70)80027-X
15. Clarke, A.D. Effects of filter internal reflection coefficient on light absorption measurements made using the integrating plate method. *Appl. Optics*, 1982, **21**(16), 3021-3031. doi:10.1364/AO.21.003021
16. Xiaobin, L. & Wallace, J.S. In-cylinder measurement of temperature and soot concentration using the two-color method. *SAE Transact., JSTOR*, 1995, **104**(3), 1480–1490.
17. Gu K.; Zhang Y. & Qiao, J. Vision-based monitoring of flare soot, *IEEE Transact. Instrument. Measure.*, 2020, **69**(9), 7136-7145. doi: 10.1109/TIM.2020.2978921.
18. Manoel J.A.L.; Milton K.S.; Oziel R.M.; Tayane A.F.; Ronaldo, C.F.; Boaventura, F.R. & Fábio, R.P.R. Spot test for fast determination of hydrogen peroxide as a milk adulterant by smartphone-based digital image colorimetry, *Microchem. J.*, 2020, **157**, 105042. doi: 10.1016/j.microc.2020.105042.
19. Oveis, H.; Igathinathane, C.; Doetkott, C.; Bajwa, S.; Nowatzki, J. & Seyed, A.H.E. Chlorophyll estimation in soybean leaves infield with smartphone digital imaging

and machine learning, *Comput. Electron. Agricult.*, 2020, **174**, 105433.
doi: 10.1016/j.compag.2020.105433.

20. Zhao, B.; Zhang, Y.; Duan, A.; Liu, Z.; Xiao, J.; Liu, Z.; Qin, A.; Ning, D.; Li, S. & Ata-Ul-Karim, S.T. Estimating the growth indices and nitrogen status based on color digital image analysis during early growth period of winter wheat. *Front. Plant Sci.*, 2021, **12**, 619522. doi: 10.3389/fpls.2021.619522
21. Ivković, R. New model of partial filtering in implementation of algorithms for edge detection and digital image segmentation. Univerzitet u Prištini, Fakultet tehničkih nauka, Kosovska Mitrovica, Serbia, 2019. (PhD Thesis).
22. Brownrigg, D.R.K. The weighted median filter. *Commun. ACM*, 1984, **27**(8), 807-818. doi:10.1145/358198.358222
23. Astola, J.; Haavisto, J.P.; Neuvo, Y. Vector median filters. *IEEE Proceed. Image*, 1990, **78**(4), 678-689. doi:10.1109/5.54807
24. Ivković, R.; Milošević, I.; Gara, B. & Petrović, M. Analysis of quality of nonlinear filters by removing salt & pepper noises. *In* YU INFO 2014, Serbia, Kopaonik, 2014.
25. Ivković, R.; Petrović, M.; Daković, B.; Jakšić, B. & Milošević, I. Segmentation and classification of bi-rads medical images with the imaging biomarkers according to level of detail. *Tehnički vjesnik*, 2020, **27**(2), 527-534. doi:10.17559/TV-20181221151205
26. Ivković, R. & Kopanja, L. Hibridni metod za detekciju ivica na TEM slikama nanočestica, *Zaštita materijala*, 2018, **59**(1), 21-30. doi:10.5937/ZasMat1801021I
27. Ivković, R.; Milošević, I.; Petrović, M.; Spalević, P.; Panić. S. Image Segmentation by Sobel Edge Detection Algorithm - Mosaic Method, *In* Sinteza 2018 International Scientific Conference on Information Technology and Data Related Research, Singidunum University, Belgrade, Serbia, 2018. doi:10.15308/Sinteza-2018-189-196
28. Apostolakis, G. & Kaplan, S. Pitfalls in risk calculations. *Reliability Eng.*, 1981, **2**(2), 135-145. doi:10.1016/0143-8174(81)90019-6
29. Viscusi, W.K. The challenge of punitive damages mathematics. *J. Legal Stud.*, 2001, **30**(2), 313-350. doi:10.1086/322059

CONTRIBUTORS

Dr Ratko Ivković obtained his PhD degrees in Electronic and Computer Engineering from the Faculty of Technical Sciences, Department of Electronics and Telecommunications Engineering, Serbia. His expertise lies in filter design, segmentation, image similarity techniques, image restoration, and noise reduction in digital images.